Kink-formation kinetics and submonolayer density of magic two-dimensional islands in molecular beam epitaxy

Sergey Filimonov and Yuri Hervieu*
Department of Physics, Tomsk State University, 634050 Tomsk, Russia
(Received 21 September 2009; published 23 November 2009)

The nucleation and growth of compact two-dimensional islands having a regular shape and edges consisting of atomically straight kink-free segments is studied analytically and with kinetic Monte Carlo (KMC) simulations. In the analytical model the islands grow by a cyclic process of deposition of single atomic rows along the island edges. Two ends of an incomplete row are the kink sites where adatoms incorporate into the crystal. Adatoms attached to the island edge are able to migrate along the edge and detach back to the terrace before reaching the kinks. Completion of the rows corresponds to a sequence of the magic island sizes. It is assumed that a one-dimensional nucleus of the next atomic row (a pair of kinks) forms when two adatoms meet each other at the edge of the magic island. It follows from the model that at certain growth conditions the island density is independent of the deposition flux and increases with the increasing growth temperature. The predictions of the analytical model are in good agreement with results of KMC simulations. Computer simulations also show that the island size distribution gradually changes with the increasing detachment probability from the monomodal distribution with a peak around the mean island size to a sequence of monotonously decreasing peaks at magic sizes.

DOI: 10.1103/PhysRevE.80.051603 PACS number(s): 81.15.Aa, 68.55.A−, 68.35.Fx

I. INTRODUCTION

The nucleation and growth of two-dimensional (2D) islands at the early stage of molecular beam epitaxy has been studied intensively in the last decades due to its importance for the epitaxial technology and also because this process represents an interesting example of far-from-equilibrium statistical physics [1–3]. Many experimental and theoretical efforts have been made to relate the island density and island size distribution with parameters of the underlying atomic processes (see [4] for a recent review). Theories based on the mean-field rate equation approach [5,6] appeared to be very successful in describing behavior of the mean density of 2D islands. Predictions of these theories are widely used for interpretation of the experimental dependences of the 2D island density on the deposition flux and substrate temperature and for extraction of important microscopic parameters of the growth process [7–11].

In a typical picture of atomic processes considered in the nucleation models atoms are deposited on the surface at a rate F and migrate on the surface with a temperature-dependent diffusion coefficient D. Eventually a migrating adatom either meets another adatom to form a dimer or attaches to an existing cluster of $s \geq 2$ atoms (2D island). There are two main approaches to take into account detachment of atoms from the islands [12]. The first assumes the existence of a critical nucleus of size i^* such that beyond this size, i.e., at $s > i^*$, the islands are stable against decay and grow by irreversible attachment of adatoms. On the contrary, the subcritical ($s \leq i^*$) clusters are assumed to be in quasiequilibrium with the adatom gas, so that the Walton relation can be applied to express the density of the critical nuclei via the adatom density, diffusion coefficient, and energy of dissociation of the nucleus [13].

The second approach permits detachment of atoms from the islands of any size. It is noteworthy that the detachment rate is usually assumed to be independent of the current island configuration, although it may depend on the island size [14–16]. The introduction of the size-dependent detachment rate represents an important generalization of the nucleation models; however, in certain cases not only the island size but also the island structure has to be taken into account.

An important example in that respect is the nucleation and growth of 2D islands on reconstructed surfaces. So, nucleation of 2D islands on Si(111) and Si(001) surfaces is influenced by the presence of the surface reconstruction and represents a multistage process which involves an intermediate stage of formation of relatively stable nonepitaxial clusters [17–19]. Moreover, the processes of adatom incorporation into 2D islands may be more complicated than those considered in the traditional approach. For example, 2D Si and Ge islands on the Si(111)-7×7 surface typically develop a *kinetically* limited triangular shape and, at certain growth conditions, have predominantly magic sizes of the squares of integer numbers of half unit cells of the 7×7 structure [20–22]. This indicates the row-by-row mechanism of the island growth and slow rate of formation of kinks at the island edge as compared to the rate of propagation of the kink along the edge.

The formation of kinks at far-from-equilibrium conditions occurs for the most part by the one-dimensional (1D) nucleation mechanism [23–25] which presumes the meeting of two or more adatoms at the step edge. The necessary condition for the rate of 1D nucleation to be slow is that an adatom attached to the straight (without kinks) island edge with high probability detaches back to the terrace [26]. On the contrary, fast and irreversible propagation of kinks means that acts of detachment of atoms from the island containing one or more kinks at its edge are relatively rare. Evidently, the detachment rate in this case depends crucially on the island configuration.

*hervieu@elefot.tsu.ru

The growth of 2D islands with a configuration-dependent detachment of atoms has been addressed by Mazzitello *et al.* [27,28] subject to the case of chains of Si dimers representing quasi-1D Si islands on Si(001). They assumed that no detachment of atoms is possible from islands with an even number of atoms (the dimer at the end of the chain is stable) whereas detachment of atoms from islands with an odd number of atoms (i.e., detachment of lonely atoms from the ends of the chains) occurs with some probability. The results obtained with the rate equation model of Refs. [27,28] clearly demonstrate that dependences of the island density on the temperature and deposition rate can be strongly influenced by the incorporation mechanisms specific to the growth on reconstructed surfaces and that they can be very different from those predicted by the standard theories.

The growth of dimer chains is a particular case of the growth of magic islands where the magic sizes are given by a sequence of even numbers. However, the model developed in Refs. [27,28] refers to so-called point-island models [4,29] which do not take into account the influence of varying edge length on the adatom attachment/detachment rates. While in the case of the dimer chains the point-island approximation seems to be reasonable (the length of the active segment of a dimer chain remains constant during growth), generally, the effect of the varying island perimeter should not be neglected.

In the present paper we develop a simple model of growth of spatially extended magic 2D islands in the case of complete condensation of atoms arriving on the crystal surface from the molecular beam. Our model predicts that in the limit of large values of D/F and at sufficiently high rates of detachment of adatoms from the edges of the magic islands the island density N is independent of the deposition flux (in accord with the results of Ref. [27]) and increases directly proportional to the increasing detachment probability P (and hence increases with the increasing growth temperature). These scaling relations are shown to hold both in the case of fast and slow migration of adatoms along the island edge. The dependence $N \sim P$ obtained with our model is steeper than the dependence $N \sim P^{1/2}$ predicted for dimer chains [27] which is due to the impact of the island size on the rate at which an adatom escapes from the island after detachment. The analytical predictions are in good qualitative agreement with the results of kinetic Monte Carlo (KMC) simulations with realistic model parameters. The KMC simulations also demonstrate gradual transition with increasing P from the monomodal distribution with a peak around the mean island size to the series of peaks at magic sizes.

II. MODEL

A. Row-by-row growth mechanism

We will consider nucleation of 2D islands assuming that the critical nucleus size $i^*=1$; i.e., a pair of atoms form the minimal stable 2D island. The islands are assumed to be immobile and island coalescence is not taken into account. Under these assumptions the density of adatoms, n_1, and the total density of islands, N, evolve according to the following set of rate equations:

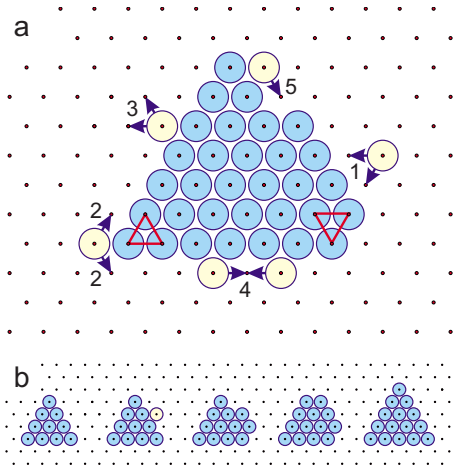

FIG. 1. (Color online) (a) Atomic processes at the island edge involved in the model: (1) attachment of an adatom to the straight edge segment, (2) migration of the edge adatom along the island edge segment and around the island corner, (3) detachment of the edge adatom from the edge to the terrace, (4) nucleation of a 1D island at one of the straight edge segments, and (5) adatom incorporation into the kink site at the end of the 1D island. (b) One cycle of the row-by-row island growth.

$$\frac{dn_1}{dt} = F - 2\sigma_1 D n_1^2 - G, \tag{1}$$

$$\frac{dN}{dt} = \sigma_1 D n_1^2, \tag{2}$$

where σ_1 is the adatom capture number and G is the net flux of adatoms incorporating into the islands. Note that throughout the paper all lengths are in atomic units. The equations above are universal in the sense that very different kinetic scenarios of the island growth can be modeled provided that the appropriate expressions for the incorporation flux G are available.

In the present work we concern the growth of magic 2D islands, which keep their shape and grow by the row-by-row mechanism sketched in Fig. 1(b). By this mechanism the deposition of every new atomic row at the island edge occurs in two stages. The first stage is the nucleation of a 1D island at the straight (without kinks) segment of the edge of the 2D island after the expectation time t_{nuc}. Two ends of the 1D island provide the kink sites where migrating adatoms may incorporate into the crystal. Attachment of adatoms increases the length of the 1D island, so, finally, it spreads over the whole segment. This second stage of the new row formation takes the mean time t_{gr}. It is essential that no other 1D islands appear during the time t_{gr}. As the crystalline row along the edge segment completes, the cycle of the 1D nucleation and growth repeats again. Since the island shape is conserved, completion of the rows corresponds to a sequence of the magic island sizes m_l $(l=1,2,3,\ldots)$. For instance, for monolayer triangular islands on a triangular lattice, $m_l=(l+1)(l+2)/2$ and l has a sense of the side length of the triangle in atomic units.

On the atomic scale the row-by-row growth of a 2D island involves the following atomic processes depicted in Fig. 1(a): (1) attachment of adatoms to the straight edge segments; (2) migration of the edge adatoms along the island edge segments and around the island corners; (3) detachment of the edge adatoms from the edge to the terrace; (4) nucleation of a 1D island at one of the straight edge segments; (5) adatom incorporation into the kink sites at the ends of the 1D island. For the sake of simplicity we assume hereafter that the edge dimer is stable and represents the minimal 1D island. In addition, no detachment of the atoms embedded into the island edge is allowed and no atom can detach from the corner sites and kink positions during the time of growth.

The incorporation flux G can be divided into two contributions. The first one G_{pre} is the flux of adatoms incorporating into the "premagic" islands, i.e., islands smaller than the minimal magic island. This contribution is of the order of the island nucleation rate $\sigma_1 D n_1^2$ and it is typically small at the steady-state regime of growth (see Sec. II D for details).

The second contribution G_Σ is the net flux of adatoms incorporating into all other islands. To estimate G_Σ let us note that the mean rate of adatom incorporation into a 2D island during one cycle of the row-by-row growth, i.e., during the island growth from one magic size m_l to another m_{l+1}, is given by the number of consumed adatoms divided by the cycle duration: $(m_{l+1}-m_l)/(t_{nuc,l}+t_{gr,l})$ [30]. Then in the case of a slow rate of formation of kinks ($t_{nuc,l} \gg t_{gr,l}$), where the majority of 2D islands are of the magic sizes, one gets

$$G_\Sigma \approx \sum_l (m_{l+1}-m_l)\omega_{nuc,l} N_{m_l}, \tag{3}$$

where N_{m_l} is the density of magic islands of size m_l and $\omega_{nuc,l}=1/t_{nuc,l}$ is the rate of formation of the stable 1D nucleus at the edge of the magic island of size m_l.

B. Time scales

To calculate $\omega_{nuc,l}$ we apply the time scale arguments similar to that used in statistical theories of second-layer nucleation [31,32] and atom recombination on interstellar dust grains [33]. Similarly to the processes described in Refs. [31–33] the 1D nucleation at the island edge considered in the present paper is essentially a two-particle process because when the majority of 2D islands are of the magic sizes the probability to find a lonely edge adatom or a kink is small. Here the 1D nucleation proceeds in the fluctuation-dominated regime [32] which may be described with the theory of Refs. [31–33].

Following Refs. [31–33] we express the nucleation rate as $\omega_{nuc,l}=\omega^+_{m_l} P_l P_{enc,l}$, where $\omega^+_{m_l}$ is the frequency of attachment of adatoms to the edge of the magic island, P_l is the probability that an adatom attached to the edge will not leave the island before arrival of the next adatom, and $P_{enc,l}$ is the probability that two adatoms, once present at the edge simultaneously, will meet before one of them leaves the island. The probability P_l can be written down as [31,32]

$$P_l = \frac{t_{res,l}}{t_{res,l}+\Delta t_{m_l+1}} \approx \frac{t_{res,l}}{\Delta t_{m_l+1}}, \tag{4}$$

where $t_{res,l}$ is the residence time of a lonely adatom at the edge of the magic island and Δt_{m_l+1} is the expectation time of attachment of the next adatom to the "magic plus one atom" island: $\Delta t_{m_l+1}=1/\omega^+_{m_l+1}$.

Passing on to the estimation of the residence and attachment times, one has to point out an important and nontrivial difference between the consequences of detachment of an adatom from the island edge and desorption of an adatom from the surface of an interstellar dust grain [33] or descending of an adatom from the top of the 2D island [31,32]. In the latter cases an adatom leaves the "reactive surface" forever whereas an adatom detached from the island edge always has chances to reattach. For this reason we put $t_{res,l}$ to be the inverse of the rate γ_{m_l+1} at which an adatom *escapes* from the island of the size m_l after detachment [14]: $t_{res,l}=1/\gamma_{m_l+1}$ and use the following expressions for the attachment frequencies: $\omega^+_{m_l}=\sigma_{m_l} D n_1$ and $\omega^+_{m_l+1}=\sigma_{m_l+1} D n_1$, where σ_{m_l} is the island capture number. This choice guarantees that calculating the nucleation rate we are dealing with two different adatoms.

To proceed we, following Bales and Zangwill [14], put the escape rate γ_{m_l+1} to be the inverse of the island perimeter (which scales as $m_{l+1}-m_l$): $\gamma_{m_l+1} \sim \sigma_{m_l}\omega^-_{m_l+1}/(m_{l+1}-m_l)$. Note that the microscopic detachment rate $\omega^-_{m_l+1}$ is here the rate of detachment of a lonely adatom at the edge of the magic island. This rate is independent of the island size and may be described by a simple Arrhenius relation: $\omega^-_{m_l+1}=\omega^- \sim D e^{-E_b/kT}$, where E_b is the binding energy of an adatom to the atomically straight edge of the island. Using these definitions one obtains

$$\omega_{nuc,l} = \frac{(m_{l+1}-m_l)\sigma_{m_l+1}(D n_1)^2 P_{enc,l}}{\omega^-}. \tag{5}$$

It remains to calculate the encounter probability $P_{enc,l}$. Let us denote the probability that two adatoms encounter at the edge after the first attempt by $P^1_{enc,l}$. If the first attempt fails the adatoms can try again until one of them escapes from the island capture zone after detachment. Then the encountering probability can be expressed as

$$P_{enc,l} = P^1_{enc,l} + (1-P^1_{enc,l})P^*_{enc,l}, \tag{6}$$

where $P^*_{enc,l}$ is the probability that the adatoms will meet after the second, third, etc. attempts. The probability $P^*_{enc,l}$ obeys the recurrent relation

$$P^*_{enc,l} = (1-p_{esc,m_l})[P^1_{enc,l} + (1-P^1_{enc,l})P^*_{enc,l}], \tag{7}$$

where p_{esc,m_l} is the probability that an adatom escapes from the island capture zone after detachment [16], which can be defined as $p_{esc,m_l}=\gamma_{m_l+1}/\omega^-_{m_l+1}=\chi\sigma_{m_l}/\Gamma_{m_l}$, where Γ_{m_l} is the island perimeter and χ is the geometrical factor order unity.

To estimate $P^1_{enc,l}$ let us note that there exist two ways for adatoms to encounter at the island edge. First, an adatom arriving at the island edge can hit directly the edge sites neighboring to the adatom arrived previously. The probabil-

ity of this event is approximately $2/\Gamma_{m_l}$. The second possibility is that the adatoms meet in the course of migration along the edge. A simple estimate of the relevant probability can be obtained if we immobilize one of the migrating adatoms and assume that there is no additional barrier for rounding the island corners. Then the adatom encountering probability is equal to the probability that an adatom attached to the step edge between two kinks separated by the distance Γ_{m_l} reaches one of the kinks before detachment. The latter probability was estimated in Ref. [34] as $f(q_{m_l}) \approx \tanh(q_{m_l})/q_{m_l}$, where q_{m_l} is the ratio of the distance Γ_{m_l} to the mean length of adatom migration along the edge. Taking both possibilities into account one gets

$$P^1_{enc,l} = \frac{2}{\Gamma_{m_l}} + \left(1 - \frac{2}{\Gamma_{m_l}}\right) f(q_{m_l}). \tag{8}$$

Then deriving $P^*_{enc,l}$ from Eq. (7) and substituting in Eq. (6) one obtains

$$P_{enc,l} = \frac{1}{1 + \chi Q_{m_l} \sigma_{m_l}}, \tag{9}$$

where

$$Q_{m_l} = \frac{1 - f(q_{m_l})}{2 + \Gamma_{m_l} f(q_{m_l})}. \tag{10}$$

In the case of fast edge migration $q_{m_l} \ll 1$ and, consequently, $f(q_{m_l}) \approx 1$. In this case, as expected, the encountering probability is close to unity. On the contrary, when the edge migration is slow $q_{m_l} \gg 1$ and $f(q_{m_l}) \ll 1$. Then $P_{enc,l} \approx 1/(1 + \chi \sigma_{m_l}/2)$. As can be seen, in the case of slow edge migration the encountering probability can be considerably less than in the case of fast edge migration. This has to result in the decreased rate of capture of adatoms by 2D islands and, consequently, in the increased density of the islands as compared to the case of fast edge migration.

It is important that the capture number is a slowly varying function of the island size [5]. At the same time the factor Q_{m_l} appearing in Eq. (9) varies from 0 (fast edge migration) to 1/2 (no edge migration). Hence, the encountering probability is nearly independent of the island size. This is because the decrease (with the increasing island size) in the probability for adatoms to encounter from the first attempt is compensated by the increasing residence time of adatoms at the edge and thus by the increasing chances to encounter from the second, third, etc. attempts. As a consequence, the scaling relations for adatom and island densities, derived further in the text, appear to be the same both in the case of fast and slow migration of adatoms along the island edge.

C. Scaling relations

Using Eqs. (3), (5), and (9) one can write down the net flux of adatoms incorporating into the islands of sizes equal or greater than the minimal magic size m_1:

$$G_\Sigma \sim \sum_{l \geq 1} \frac{(m_{l+1} - m_l)^2 \sigma_{m_l+1} (Dn_1)^2}{\omega^-} N_{m_l} \sim \frac{\sigma_{av} S_{av} (Dn_1)^2}{\omega^-} N_\Sigma, \tag{11}$$

where $N_\Sigma \approx \Sigma_{l \geq 1} N_{m_l}$ is the total density of islands of the sizes equal or greater than m_1. S_{av} and σ_{av} are the average size and average capture number of such islands, respectively. Note that except for the initial (transient) stage of growth contribution of the premagic islands to the total island density should be small. Therefore, N_Σ approximately equals the density N of islands of all sizes and $S_{av} N_\Sigma \approx S_{av} N \approx \theta$, where θ is the surface coverage. Then one can rewrite Eq. (11) as

$$G_\Sigma = \eta \sigma_{av} D P^{-1} n_1^2 \theta, \tag{12}$$

where $P \equiv \exp(-E_b/kT) \sim \omega^-/D$ is the detachment probability [27] and η is a constant order unity.

At the steady-state regime of growth the nucleation flux [the second term in the right part of Eq. (1)] is small as compared to the incorporation flux G. At the same time G_{pre} should be much less than G_Σ; otherwise, the depositing material will accumulate in the minimal magic islands without further growth. Then one gets the steady-state rate equations in the form

$$\frac{dn_1}{dt} \approx F - \eta \sigma_{av} D P^{-1} n_1^2 \theta \approx 0, \tag{13}$$

$$\frac{dN}{dt} = \sigma_1 D n_1^2. \tag{14}$$

Assuming constant capture numbers in Eqs. (13) and (14) one comes to the following scaling relations:

$$n_1 \sim \left(\frac{D}{F}\right)^{-1/2} P^{1/2}, \tag{15}$$

$$N \sim P. \tag{16}$$

It follows from Eqs. (15) and (16) that in the limit of high escape rates the island density is independent of the incoming flux F and *increases* with the increasing growth temperature. Such an unusual behavior of N_s was predicted earlier by Mazzitello *et al.* [27] for the growth of the dimer chains. The reason is that both the formation of the island nucleus and the incorporation of adatoms into the island (into the chain) are here the processes of the same (the second) order in adatom density—two adatoms must find each other on the terrace or at the edge of the magic island to form a stable cluster. It is worth noting that a flux-independent island density was observed for Fe inclusions in Cu(100) [35] and predicted theoretically for the surfactant-mediated growth [36] (here the increasing dependence $N(T)$ is also possible; cf. regime 2 in Ref. [36]). In these cases it is very probable that the critical nucleus size is zero [35,36], so both the nucleation and incorporation are the processes of the first order.

D. Limits of the model applicability

At this point it is worth recalling the assumptions we made in the course of derivation of scaling relations (15) and

(16) since they impose the limits of the model applicability. It has been assumed that the growth proceeds in the steady-state regime without accumulation of the deposited material in the minimal magic islands. This is only possible if $G_\Sigma \gg 2\sigma_1 D n_1^2 + G_{pre}$. To estimate G_{pre} let us note that at the steady state

$$\frac{dN_2}{dt} = \sigma_1 D n_1^2 - \sigma_2 D n_1 N_2 \approx 0, \tag{17}$$

$$\frac{dN_s}{dt} = \sigma_{s-1} D n_1 N_{s-1} - \sigma_s D n_1 N_s \approx 0, \quad (s = 3 \ldots m_1 - 1), \tag{18}$$

which means that $G_{pre} = D n_1 \Sigma_{s=2}^{m_1-1} \sigma_s N_s \approx (m_1 - 2)\sigma_1 D n_1^2$. Then using Eq. (12) for G_Σ one gets $P \ll \eta \sigma_{av} \theta / (\sigma_1 m_1)$ or, at moderate values of m_1 (say, $m_1 < 10$), $P \ll \theta$.

It has been further assumed that the magic 2D islands dominate the island size distribution which is possible in our model only at sufficiently large detachment rates. According to the estimates of Sec. II B: $t_{nuc,l} \sim \gamma_{m_l+1} / [\sigma_{m_l} \sigma_{m_{l+1}} (D n_1)^2]$. Then putting $t_{gr,l} \sim (m_{l+1} - m_l)/\omega_{m_l}^+ = (m_{l+1} - m_l)/(\sigma_{m_l} D n_1)$ one can write down the strong detachment condition $t_{nuc,l} \gg t_{gr,l}$ in the form

$$\gamma_{m_l+1} \gg (m_{l+1} - m_l) \sigma_{m_l+1} D n_1. \tag{19}$$

Recalling the expression for γ_{m_l+1} one can see that inequality (19) being attributed to the mean size islands implies $P \gg S_{av} n_1 \approx \theta n_1 / N$.

These restrictions combined with Eqs. (15) and (16) yield

$$\theta \gg P \gg \left(\frac{D}{F}\right)^{-1/3}. \tag{20}$$

A rough estimate shows that inequality (20) in fact impedes realization of scaling relations (15) and (16) at typical growth conditions. Indeed, to be sure that Eq. (20) is fulfilled for, e.g., $\theta = 0.1$ and P in the range $10^{-3} - 10^{-5}$ one needs the ratio D/F to be unrealistically large ($\sim 10^{20}$). At more realistic values of $D/F (\leq 10^{12})$ the strong detachment condition is safely fulfilled only for sufficiently large values of $P \geq 10^{-2}$. But at such large P the steady-state condition is violated: the atoms of the deposited material gather in the minimal magic islands and do not incorporate into the already existing islands. So, at typical growth conditions $N(P)$ should be a nonlinear increasing function with the maximal slope of the log-log plot less unity.

Other factors limiting applicability of Eqs. (15) and (16) come from the features of the growth process which are not taken into account in the analytical model. Note that in contrast to the width of a dimer chain the perimeter of a 2D island increases with time. The strong detachment condition given by inequality (19) may break down for eventually appearing large 2D islands (much larger than the average island size $S_{av} \approx \theta / N$). Such islands can grow in the row-by-row manner without losses of the edge adatoms.

Another important feature not taken into account in the model is the coalescence of the islands. In the case of intensive detachment this process becomes essential even at very small coverages because of more random spatial distribution of the nuclei as compared to the case of irreversible growth. Apart from decreasing island density the coalescence results in the formation of macrokinks serving as the long-living sinks for adatoms. These circumstances favor irreversible attachment of adatoms thus weakening the dependence of the island density on the detachment probability P and strengthening the dependence of the island density on the deposition flux F.

In view of the model limitations, Eqs. (15) and (16) should be considered as asymptotic scaling relations. However, as we demonstrate in the next section with KMC simulations, they provide rather good reference to understand behavior of the magic island density at typical growth conditions.

III. COMPARISON TO KMC

In this section we will check predictions of the analytical model developed in Sec. II by comparing them with the results of KMC simulations. As a reference model (hereafter, model I) we will use a standard KMC model of epitaxial growth [37], with some minor extensions made to mimic growth of triangular islands. In the model atoms are deposited onto a triangular lattice with a frequency F and allowed to perform random hops to nearest-neighbor sites with a temperature-dependent hopping rate $h_s = \nu \exp(-E_s/k_B T)$, where E_s is the activation barrier for adatom diffusion on a terrace and ν is the attempt frequency. Whenever two adatoms are found in neighboring sites they form a stable dimer, which can neither dissociate nor move. That is, the dimer is considered to be the smallest 2D island in the model, which corresponds to the critical cluster size $i^* = 1$ in terms of the atomistic nucleation theory [5]. When a migrating adatom encounters an island boundary, its behavior may depend on the orientation of the particular edge segment. On a triangular lattice one may distinguish two sets of directions which form up-pointing (type A) and down-pointing (type B) triangles in Fig. 1(a). To force the formation of triangular islands of only one type we used the following rules for the hopping of adatoms at the island edges. An adatom attached to the A-type step was allowed to migrate along the edge with the rate $h_e = \nu \exp(-E_e/k_B T)$, where E_e is the activation barrier for adatom migration along the island edge, and detach from the edge with the rate $h_{es} = \nu \exp[-(E_s + E_b)/k_B T]$. On the contrary, an atom attached to the B-type segment was immediately immobilized and joined the crystal irreversibly. Irreversible incorporation of an adatom also takes place in our simulations when the atom attaches to the kink site or meets another adatom at the island edge forming a stable edge dimer.

The second model (model II) was a point-island model. In this model each island irrespectively to the actual island size is represented by a point on the surface. A counter of the number of incorporated atoms is assigned to each point island, which we will refer to as the size of a point island. An atom attached to the point island of a magic size m_l is allowed to detach from the island with a rate $h_{es} = \nu \exp[-(E_s + E_b)/k_B T]$ which is equal to the detachment rate $\omega_{m_l+1}^-$ used

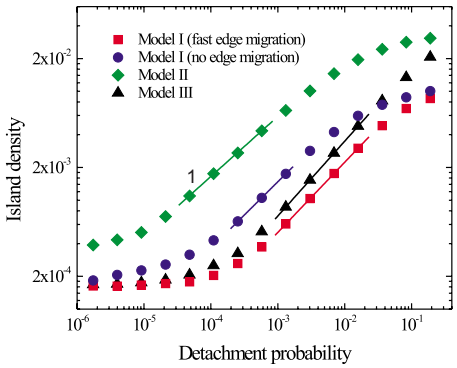

FIG. 2. (Color online) Log-log plots of the island density vs the detachment probability obtained for $T=700$ K and $F=0.2$ ML/s. The slopes of the fitting lines are 0.65 ± 0.01 (model I; fast edge migration), 0.61 ± 0.01 (model I; no edge migration), 0.55 ± 0.005 (model II), and 0.68 ± 0.01 (model III).

in the analytical model of Sec. II. An atom attached to a point island of any nonmagic size cannot leave the island anymore. By construction, the island boundary length is zero in the point-island model, so that the adatom escape rate does not depend on the island size in model II and islands cannot coalesce.

To include the effect of a nonzero island boundary length we applied an extended point-island model (model III), which is based on the same rules as the point-island model, except for the fact that adatom attachment to the island occurs not at a single point but on an imaginary line that represents the position of the island edge as if the island would be a regular triangle expanding from the nucleation point. Similar to the point-island model the island coalescence is not taken into account in the extended point model.

In all the simulations reported here the activation barrier for adatom surface diffusion was $E_s=0.6$ eV and the attempt frequency was $\nu=10^{13}$ s^{-1}. In simulations with the reference model I, if not specially stated, the barriers for migration along the island edge and for rounding the island corners were set to the same value of 0.6 eV for simplicity. The binding energy of an adatom to the step edge E_b was varied from 0.1 to 0.8 eV. At a fixed temperature of 700 K this corresponds to a variation in the detachment probability P in the range $1.7\times10^{-6}-1.9\times10^{-1}$. The simulations have been performed on a triangular lattice up to the deposit coverage of 0.1 ML. The lattice size was in the range from 1000×500 to 4000×2000 atoms. At the chosen simulation parameters this range of lattice sizes provides a good statistics for the density of 2D islands. But to achieve statistically reliable results for the density of adatoms simulations on much larger lattices are needed which is too time consuming. For this reason we report here only the simulation results obtained for islands.

Figure 2 shows the island density N as a function of the detachment probability P obtained with different KMC models at $F=0.2$ ML/s and $T=700$ K($D/F\approx2.4\times10^9$). As can be seen from Fig. 2 the extended point model (model III) yields the island densities which are much closer to the results obtained with the reference model I than the island densities obtained with the point-island model (model II). This clearly demonstrates that there is a strong impact of the island size on the adatom escape rate. The differences between the results of model I and model III are mostly due to the island coalescence, which is present in simulations done with the reference model but absent from the extended point model. When detachment probability P is small, the islands are well separated and at the early stage of growth the coalescence events are rare. Therefore, the densities obtained with those two models nearly coincide at small P. On the contrary, at large P the correlations in the island positions are lost, and in the simulations done with the reference model intensive coalescence occurs already at the very early stages of growth. This contributes to a higher island density obtained with model III than with model I. It is also seen from Fig. 2 that when the detachment probability becomes very high ($P>0.1$) the dependences $N(P)$ obtained with the point-island model and extended point model converge. This is because at such large P the steady-state condition $P\ll\theta$ (cf. Sec. II D) is violated and deposited atoms predominantly accumulate in the islands of the minimal magic size, so the difference between two models vanishes.

We also checked the impact of the edge migration on the island density. For this aim, we run model I with the edge migration barrier and corner rounding barrier being set to 10 eV, which, in fact, prohibits any edge migration and corner rounding at $T=700$ K. The points corresponding to this special case of no edge migration are shown in Fig. 2 by circles. As expected, the hindered edge migration results in a somewhat higher island density than in the case of fast edge migration at moderate values of the detachment probability P. However, both at very high and very low detachment probabilities the island density occurs to be insensitive to the edge migration.

Scaling relation (16) derived in Sec. II predicts that the island density should be directly proportional to the detachment probability in the strong detachment regime: $N\sim P$. However, as can be seen from Fig. 2, the maximal slopes of the plots obtained with model I and model III are smaller than unity. For the point-island model, where the adatom escape rate does not depend on the island size, our theory predicts a somewhat weaker dependence $N\sim P^{2/3}$. But here, again, computer simulations with model II give a value smaller than 2/3 predicted by the analytical theory. We believe that the main reason for these discrepancies is that the value of D/F at which the simulations were performed is not large enough to fulfill the strong detachment condition. Indeed, the simulations performed at ten times smaller deposition flux $F=0.02$ ML/s($D/F\approx2.4\times10^{10}$) give larger values of the slopes: 0.7 ± 0.01 (model I; fast edge migration), 0.66 ± 0.01 (model I; no edge migration), 0.72 ± 0.01 (model III), and 0.59 ± 0.01 (model II). Note that the value obtained with model I in the case of fast edge migration of adatoms is close to that in the absence of the edge migration. This supports the conclusion of Sec. III that the scaling relations should be the same in the cases of fast and slow adatom migration along the edge.

Figure 3 presents the scaled island size distributions obtained with model I at $F=0.2$ ML/s, $T=700$ K, and three different values of the step edge binding energy E_b. The size distribution obtained at $E_b=0.65$ eV [Fig. 3(a)] resembles

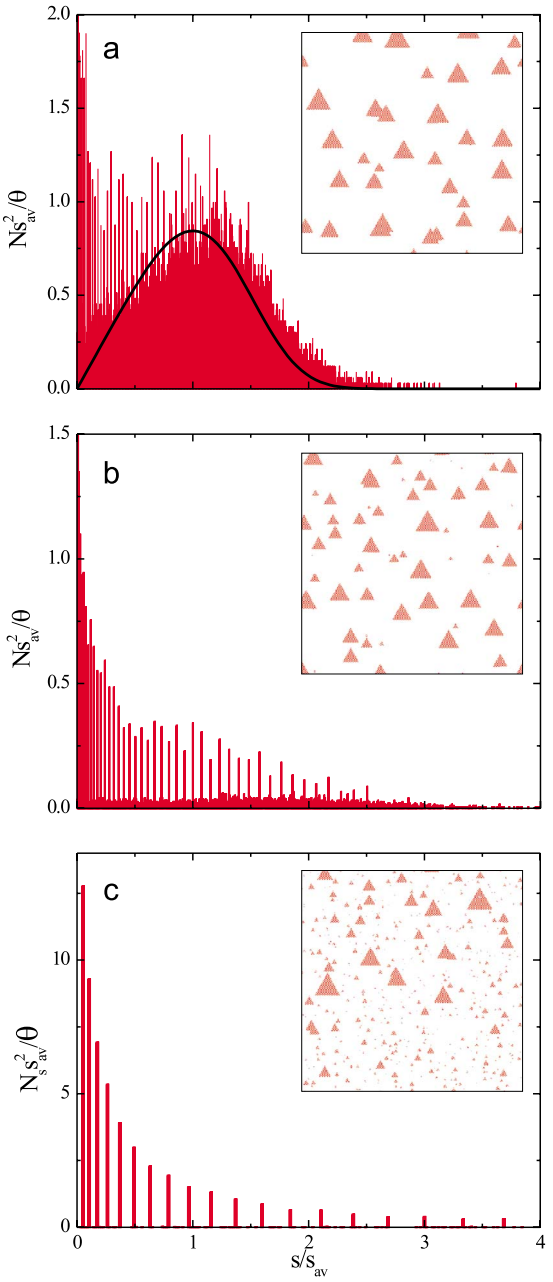

FIG. 3. (Color online) Scaled island size distributions obtained for $T=700$ K, $F=0.2$ ML/s, and for the binding energy E_b of (a) 0.65 eV, (b) 0.5 eV, and (c) 0.3 eV. The scaling function of Amar and Family [38] is shown in (a) by a solid line. The insets show 500×500 snapshots of the simulated surface.

the standard monomodal distribution with a peak around the mean island size [38], but one can observe also some peaks at magic sizes due to a nonzero probability of detachment at $E_b=0.65$ eV. With decreasing binding energy down to $E_b=0.5$ eV this multipeak distribution becomes much more pronounced [Fig. 3(b)] though the total densities of magic and nonmagic islands are comparable. Finally, at $E_b=0.3$ eV the density of nonmagic islands becomes negligible and the island size distribution represents a well-defined series of peaks at magic sizes [Fig. 3(c)]. The height of the peaks decreases monotonously with the increasing magic

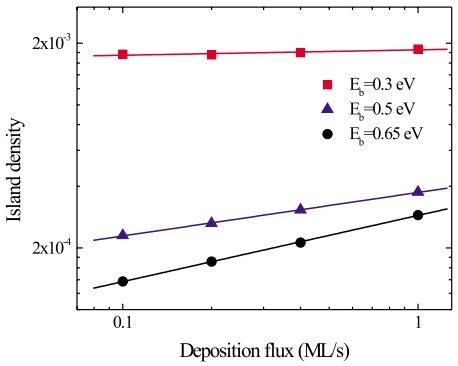

FIG. 4. (Color online) Log-log plots of the island density vs the deposition flux obtained for $T=700$ K and for three different values of the binding energy.

size. Evidently, appearance of the "magic" peaks in the island size distribution is caused by the increased rate of the detachment of edge adatoms from the "magic plus one atom" islands. The appearance of such a decaying island size distribution is in agreement with a criterion suggested by Albao *et al.* [39]. According to Ref. [39] a large population of small islands forms if the nucleation rate (the flux of adatoms into the premagic islands) dominates the aggregation rate (the flux of adatoms into the magic islands) at the crossover from a transient (initial) regime to a steady-state regime. This is exactly what we observed with KMC simulations at small E_b.

Figure 4 shows the log-log plots of the island density versus the deposition flux obtained with model I at $T=700$ K and at the same values of E_b as in Fig. 3. As can be seen the flux dependence can be well approximated by a power function $N\sim F^{\chi}$. At $E_b=0.65$ eV the exponent χ is very close to the standard value 1/3 predicted for irreversible adatom incorporation. But already at $E_b=0.5$ eV it drops to 0.21. At even smaller binding energy of 0.3 eV simulations yield $\chi\approx0.03$; i.e., the island density becomes virtually independent of the deposition flux in excellent agreement with predictions of the analytical theory of Sec. II for the strong detachment limit.

In Fig. 5 we show the Arrhenius plots of the island densities obtained with model I at $F=0.2$ ML/s and at the same values of E_b as in Figs. 3 and 4. As can be seen from Fig. 5 the decreasing temperature dependence characteristic for the strong bonding of adatoms to the step edges ($E_b=0.65$ eV) is replaced by an increasing $N(T)$ dependence at $E_b=0.5$ and 0.3 eV. That is, the simulated temperature dependence of the island density is in qualitative agreement with the analytical theory.

IV. SUMMARY

In the present work we studied theoretically peculiarities of nucleation and growth of compact 2D islands having a regular shape and edges consisting of atomically straight kink-free segments. Such islands tend to maintain their shape and grow by a two-stage row-by-row mechanism which involves (1) nucleation of a new atomic row (1D island) at the

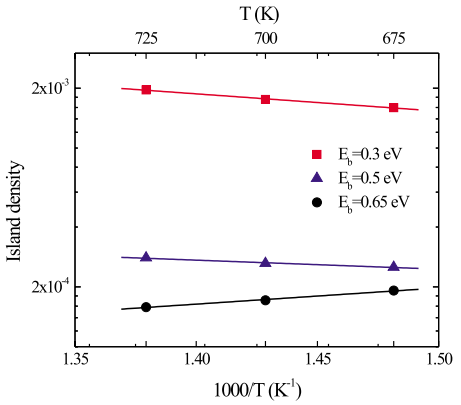

FIG. 5. (Color online) Arrhenius plot of the island density obtained for $F=0.2$ ML/s and for three different values of the binding energy.

island edge and (2) spreading of the nucleated 1D island along the edge. When the kink-free edge segments cannot provide strong traps for migrating adatoms, the 1D nucleation may be the limiting stage of the row-by-row island growth. In this case of strong detachment of edge adatoms, the islands on the surface have predominantly magic sizes corresponding to the complete regular island shape.

The central result of our study is scaling relations (15) and (16) for the adatom density and density of magic 2D islands in the strong detachment limit. These expressions were obtained assuming the simplest scenario of the 2D nucleation through the formation of immobile stable dimers on the terraces (the critical nucleus size $i^*=1$). It has been shown that the derived scaling relations hold both in the case of fast and slow migration of adatoms along the island edge. According to Eq. (16) the density of magic islands N does not depend on the deposition flux and increases with the increasing detachment probability P and, therefore, increases with the increasing growth temperature. These predictions are in qualitative agreement with the results of an earlier study of growth of dimer chains [27]. However, our model predicts a steeper dependence of N on $P(N\sim P)$ as compared to the results of Ref. [27] where the relation $N\sim P^{1/2}$ has been derived. This difference is due to the impact of the island size on the adatom escape rate which is absent from the point-island model of Ref. [27].

Scaling relations (15) and (16) were obtained under rather severe restrictions on the detachment probability P given by inequality (20). In addition, intense coalescence of the islands which takes place already at the early stage of deposition at high P was not taken into account in our analytical model. To check the predictions of this model we have performed KMC simulations of the magic island growth. Our simulations have shown that, although Eqs. (15) and (16) are not exactly fulfilled in simulations with realistic model parameters, they can serve as a good reference to understand behavior of the magic island density at typical growth conditions.

The KMC simulations also showed that the island size distribution gradually changes with the increasing P from the monomodal distribution with a peak around the mean island size to the well-defined series of peaks at magic sizes. It demonstrates that the experimentally observed multipeak island size distribution [20] is not necessarily related to the presence of an additional barrier for adatom incorporation, as it was assumed in earlier KMC simulations of the magic island growth [20,21]. Instead, the adatom incorporation can be hindered by a weak adatom bonding to the kink-free island edges. The change in the island size distribution correlates strongly with the transition to unusual dependences of the island density on the temperature and deposition flux.

ACKNOWLEDGMENT

This work was supported by the Russian Foundation for Basic Research under Grant No. 08-02-00507.

[1] J. A. Venables, *Introduction to Surface and Thin Film Processes* (Cambridge University Press, Cambridge, 2000).
[2] A. Pimpinelli and J. Villain, *Physics of Crystal Growth* (Cambridge University Press, Cambridge, 1998).
[3] T. Michely and J. Krug, *Islands, Mounds and Atoms: Patterns and Processes in Crystal Growth Far from Equilibrium* (Springer, Heidelberg, 2004).
[4] J. W. Evans, P. A. Thiel, and M. C. Bartelt, Surf. Sci. Rep. **61**, 1 (2006).
[5] J. A. Venables, G. D. T. Spiller, and M. Hanbücken, Rep. Prog. Phys. **47**, 399 (1984).
[6] S. Stoyanov and D. Kashchiev, in *Current Topics in Material Sciences*, edited by E. Kaldis (North-Holland, Amsterdam, 1981), Vol. 7, p. 69.
[7] J. A. Stroscio and D. T. Pierce, Phys. Rev. B **49**, 8522 (1994).
[8] B. Voigtländer, A. Zinner, T. Weber, and H. P. Bonzel, Phys. Rev. B **51**, 7583 (1995).
[9] H. Brune, G. S. Bales, J. Jacobsen, C. Boragno, and K. Kern, Phys. Rev. B **60**, 5991 (1999).
[10] V. Cherepanov, S. Filimonov, J. Mysliveček, and B. Voigtländer, Phys. Rev. B **70**, 085401 (2004).
[11] H. Rauscher, J. Braun, and R. J. Behm, Phys. Rev. Lett. **96**, 116101 (2006).
[12] C. Ratsch and J. A. Venables, J. Vac. Sci. Technol. A **21**, S96 (2003).
[13] D. Walton, J. Chem. Phys. **37**, 2182 (1962).
[14] G. S. Bales and A. Zangwill, Phys. Rev. B **55**, R1973 (1997).
[15] I. T. Koponen, M. O. Jahma, M. Rusanen, and T. Ala-Nissila, Phys. Rev. Lett. **92**, 086103 (2004).
[16] M. Petersen, C. Ratsch, R. E. Caflisch, and A. Zangwill, Phys. Rev. E **64**, 061602 (2001).
[17] H. Tochihara and W. Shimada, Surf. Sci. **296**, 186 (1993).
[18] Raj Ganesh S. Pala and F. Liu, Phys. Rev. Lett. **95**, 136106 (2005).
[19] S. Filimonov, V. Cherepanov, Yu. Hervieu, and B. Voigtländer, Phys. Rev. B **76**, 035428 (2007).

[20] B. Voigtländer, M. Kästner, and P. Šmilauer, Phys. Rev. Lett. **81**, 858 (1998).
[21] J. Mysliveček, T. Jarolímek, P. Šmilauer, B. Voigtländer, and M. Kästner, Phys. Rev. B **60**, 13869 (1999).
[22] B. Voigtländer, Surf. Sci. Rep. **43**, 127 (2001).
[23] V. V. Voronkov, Kristallografiya **15**, 13 (1970) [Sov. Phys. Crystallogr. **15**, 8 (1970)].
[24] R. E. Caflisch, W. E, M. F. Gyure, B. Merriman, and C. Ratsch, Phys. Rev. E **59**, 6879 (1999).
[25] A. A. Chernov, J. Mater. Sci.: Mater. Electron. **12**, 437 (2001).
[26] The slow rate of 1D nucleation can also be caused by an extra barrier for adatom attachment to the kink-free step edge positions; see Refs. [20–22].
[27] K. I. Mazzitello, H. O. Mártin, and C. M. Aldao, Phys. Rev. E **69**, 041604 (2004).
[28] K. I. Mazzitello, C. M. Aldao, and H. O. Mártin, Phys. Rev. E **74**, 011602 (2006).
[29] M. C. Bartelt and J. W. Evans, Phys. Rev. B **46**, 12675 (1992).
[30] S. N. Filimonov and Yu. Yu. Hervieu, Int. J. Nanosci. **6**, 237 (2007).
[31] J. Krug, P. Politi, and T. Michely, Phys. Rev. B **61**, 14037 (2000).
[32] J. Krug, Eur. Phys. J. B **18**, 713 (2000).
[33] J. Krug, Phys. Rev. E **67**, 065102(R) (2003).
[34] S. N. Filimonov and Yu. Yu. Hervieu, Surf. Sci. **553**, 133 (2004).
[35] D. D. Chambliss and K. E. Johnson, Phys. Rev. B **50**, 5012 (1994).
[36] S. Liu, S.-Y. Wu, and Z. Zhang, Surf. Sci. **486**, 208 (2001).
[37] S. Clarke and D. D. Vvedensky, Phys. Rev. Lett. **58**, 2235 (1987).
[38] J. G. Amar and F. Family, Phys. Rev. Lett. **74**, 2066 (1995).
[39] M. A. Albao, M. M. R. Evans, J. Nogami, D. Zorn, M. S. Gordon, and J. W. Evans, Phys. Rev. B **72**, 035426 (2005).